



# SIMULATIONS OF HIGH-Z GALAXY OBSERVATIONS WITH AN E-ELT/MOS

Mathieu Puech<sup>1a</sup>, Karen Disseau<sup>1</sup>, Laura Pentericci<sup>2</sup>, and the MOSAIC consortium

<sup>1</sup> GEPI, Observatoire de Paris, CNRS-UMR8111, Univ. Paris-Diderot, 5 place Janssen, 92190 Meudon, France

<sup>2</sup> INAF, Osservatorio Astronomico di Roma, via di Frascati 33, 00040 Monte Porzio Catone, Italy

**Abstract.** We present simulated observations of two important science cases for the 39m E-ELT, i.e., the spatially-resolved properties of distant galaxies and the detection of very high- $z$  galaxies. These simulations are currently used to constrain the top level requirements of MOSAIC, which is a new MOS concept for the E-ELT. MOSAIC largely builds on two E-ELT instrument phase A studies, namely EAGLE, an MOAO-fed NIR multi-IFU spectrograph and OPTIMOS-EVE, a GLAO-limited fiber-fed NIR spectrograph. We briefly illustrate how simulations of galaxy observations are currently used to constrain the instrument conceptual design, and in particular simulations of the detection of UV interstellar lines in very distant (i.e.,  $z \geq 6$ ) galaxies.

## 1 The (urgent) need for a MOS on the E-ELT

The multi-object spectrographs are currently the workhorse instruments of the 8-10 meter class observatories. These facilities are indeed very efficient in providing extensive spectroscopic follow-up observations to both ground-based and space-borne imaging surveys. With the advent of deeper surveys from, e.g., the HST and VISTA, there are a plethora of spectroscopic targets which are already beyond the sensitivity limits of current facilities. This wealth of targets will grow even more rapidly in the coming years, e.g., after the completion of ALMA, the launch of the JWST and EUCLID, and the advent of the LSST. Thus, one of the key requirements underlying plans for the next generation of ground-based telescopes, the Extremely Large Telescopes (ELTs), is for even greater sensitivity for optical and infrared (IR) spectroscopy. Moreover, with only three ELTs planned, the need to make efficient use of their focal planes becomes even more compelling than at current facilities given the large construction and operational costs. More specifically, the future European ELT 39m telescope, the E-ELT, will have a typical  $\sim 40$  arcmin<sup>2</sup> patrol FoV, which will provide hundreds of faint targets to be studied spectroscopically. Exploiting these densities efficiently calls for a MOS relatively early in the E-ELT instrument suite.

## 2 The ELT-MOS Science Cases

Since the end of the ESO instrument phase A studies, we revisited the science cases for an ELT-MOS. This process was stimulated by several international and national meetings held in Amsterdam (in Oct. 2012) and in several European countries (i.e., UK, Italy, Brazil and

---

<sup>a</sup> mathieu.puech@obspm.fr

Netherlands). The conclusions of these meetings were summarized in a White Paper available on astro-ph (Evans et al. 2012).

We identified six prominent science cases:

- SC1: First light and spectroscopy of the most distant galaxies;
- SC2: Spatially-resolved spectroscopy of high- $z$  galaxies;
- SC3: Role of high- $z$  dwarf galaxies in galaxy evolution;
- SC4: Tomography of the IGM;
- SC5: Resolved stellar populations beyond the Local Group;
- SC6: Galaxy archaeology with metal-poor stars.

Investigating these science cases (SCs) led us to define a top level requirement (TLR) matrix, which list the required spectral and spatial resolution, multiplex, end spectral bandwidth for each of these SCs. The next step is to prioritize the requirements and iterate with technical and operational feasibility. To assist in the required trade-off (e.g., spectral bandwidth vs. multiplex vs. spatial resolution), we decided to run end-to-end MOS simulations over a large range of parameters. During the E-ELT instrument phase A studies, we developed a very versatile simulation tool called `WEBSIM`. This tool was used to validate the science top level requirements of EAGLE (Cuby et al. 2010) and OPTIMOS-EVE (Hammer et al. 2010). It consists in a web interface coupled to an IDL code, which allows the user to conduct full simulations of an observing mode (including AO-assisted IFUs) with realistic PSFs. A full description of `WEBSIM` can be found in Puech et al. (2010c).

### 3 MOSAIC: a MOS concept for the E-ELT

During the E-ELT instrument phase A studies, several MOS concepts were studied, amongst which EAGLE, an near infrared multi-integral field spectrograph fed by multi-object adaptive optics (MOAO, see, e.g., Hammer et al. 2004), and OPTIMOS-EVE, an optical-near infrared MOS (with IFUs or mono-aperture fibers). Since 2011, these two consortia have joined their efforts to combine the best of the two proposed concepts into a single instrument at lower cost and complexity, called MOSAIC<sup>1</sup>

The ELT-MOS White Paper (Evans et al. 2012) led the MOSAIC consortium to define two main observing modes, i.e., the High Multiplex Mode (HMM) *à la* OPTIMOS-EVE, with  $\sim 100$ -250 mono-aperture fibers with GLAO/seeing resolutions, and a High Definition Mode *à la* EAGLE, with  $\sim 10$  MOAO-fed IFUs with 40-80 mas sampling. The HMM mode is dedicated to the study of the integrated light emitted by the most compact sources of interest (e.g., very first galaxies, dwarf satellite galaxies), while the HDM is necessary to spatially-resolve the properties of, e.g., distant galaxies, with large enough signal-to-noise ratios. These two modes have been implemented into two preliminary concepts, which are now under evaluation by the consortium against the MOSAIC scientific top level requirements.

### 4 Simulated SC2: spatially-resolved spectroscopy of high- $z$ galaxies

This science case was simulated in detail during the E-ELT Design Reference Mission and the EAGLE phase A study (Puech et al. 2010b,a). Simulations were used to quantify the required

<sup>1</sup> Multi-Object Spectrograph for Astrophysics, Inter galactic medium studies and Cosmology

IFU pixel scale and AO correction (as quantified using the Ensquared Energy within an element of spatial resolution). These two choices result from a trade-off between spatial resolution and surface brightness limit.

A significant fraction of high- $z$  galaxies (e.g., Elmegreen et al. 2007; Puech 2010) reveal relatively thick disks with a clumpy mass distribution. Such clumps are thought to be potentially important in galaxy evolution. The primary driver for the definition of the EAGLE IFUs was spatial resolution, with the goal of spatially-resolving the internal kinematics of such clumps, which led the EAGLE consortium to adopt a spaxel size of 37.5 mas (Puech et al. 2010a). However, it is now known that the ELT-MOS will arrive at best in third position in the E-ELT instrument plan. The two first light instruments will be a near infrared camera (ELT-CAM) and a mono integral field spectrograph (ELT-IFU). ELT-IFU will provide spatial scales ranging from the diffraction limit up to  $\sim 40$  mas (Thatte et al., these proceedings). In addition, there are significant ongoing efforts in this field at VLT with AO+LGS (e.g., Newman et al. 2013). It is therefore likely that samples of a few tens or even hundreds of clumpy galaxies with good spatial resolution will be assembled by the time the ELT-MOS becomes available on sky. This means that it is probably a better niche for ELT-MOS to be optimized in terms of survey speed rather than in term of spatial resolution. The next scale of interest in galaxies is the galaxy diameter, on which the dynamical state of galaxies is imprinted. Simulations reveal that if one wants to distinguish a merger and a rotating disks at  $z\sim 4$ , spatial sampling of 50-75 mas with  $EE\sim 30\%$  are fine enough (see Fig. 1; Puech et al. 2008).

## 5 Simulated SC1: First light and spectroscopy of the most distant galaxies

The goal of this science case is to identify the sources responsible for the reionisation of the Universe at  $z\geq 6$ . We first simulated IFU observations of UV interstellar lines in  $z\sim 7$  galaxies. Such lines are used to study the inter-stellar medium and the properties of outflowing winds in these galaxies. For this, we first rescaled hydrodynamical simulations of idealized local clumpy galaxies (which is the expected morpho-kinematic state for these targets) from Bournaud et al. (2007) to the typical size (half-light radius  $R_{half}=100-225$  mas) and flux ( $J_{AB}=25-28$ ) observed in HST/WFC3 data (e.g., Grazian et al. 2012). Then, we used the Shapley et al. (2003) stacked spectrum of  $z\sim 3$  LBGs as a model for the spectral lines, resampled at  $R=4000$ , which is necessary to work between OH sky lines. We assumed an MOAO correction providing 30% of EE within  $80\times 80\text{mas}^2$ , using an EAGLE simulated Phase A PSF. From each simulated datacube, we constructed an integrated spectrum following Rosales-Ortega et al. (2012). The optimal pixel scale (in terms of survey speed or S/N) is found to be 80-120 mas (see Fig. 2). An IFU with such a sampling would allow us to reach a  $S/N=5$  in the Si II interstellar absorption line ( $\lambda=152.7$  nm) within 40 hr of integration time and down to  $J_{AB}\geq 26$ , reaching  $J_{AB}=27$  for the most compact sources.

We also simulated IFU observations of the Ly- $\alpha$  line, which is a widely used technique to detect Lyman Alpha Emitters (LAEs), an important sub-population of very high- $z$  galaxies. This time, we focused on the 121.6 nm spectral region around the Ly- $\alpha$  redshifted at  $z\sim 9$ . We modeled this line as a truncated Gaussian on the blue side, following observations of LAEs at  $z\sim 3-7$  (e.g., Steidel et al. 2003; Swinbank et al. 2007; Hu et al. 2010; Jiang et al. 2013). We assumed a constant 200 km/s blueshift of the line compared to other nebular lines, consistent with the spatially constant outflow observed by Swinbank et al. (2007) in a  $L^*$  lensed LBG at

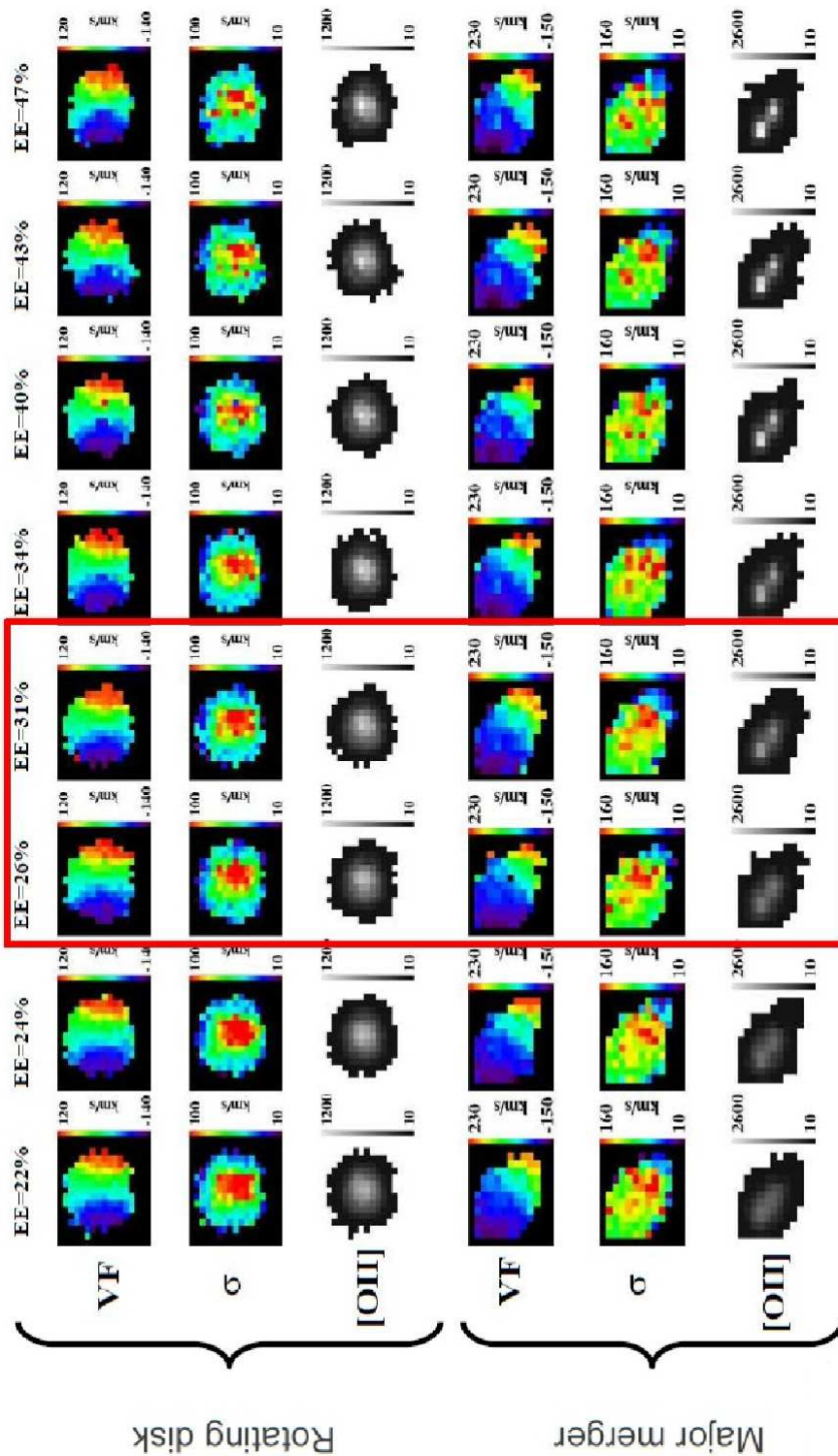


**Fig. 1.** Simulations of IFU observations (75 mas/pixel) of a rotating galaxy disk (three first rows) and a major merger (last three rows) at  $z=4$  with the E-ELT (Puech et al. 2008). In each case, the first line represent the velocity field, the second line the velocity dispersion, and the third line the [OII] emission line map (redshifted in the H band) as derived from the simulated datacubes. Each column show the result of the simulations for a different level of MOAO correction, which increases from left to right. The physical nature of the two objects can be distinguished provided that  $EE \sim 25\text{-}30\%$  within 150 mas (see details in Puech et al. 2008).

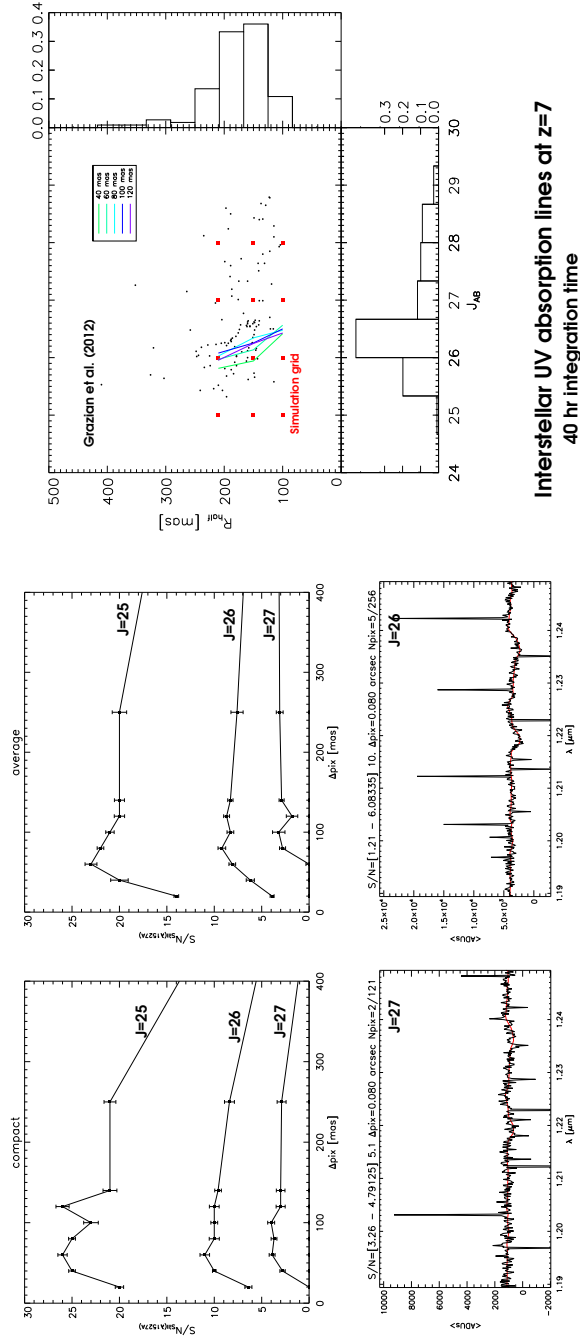


**Fig. 2.** Summary of the simulations of UV interstellar absorption lines observations at  $z \sim 7$  with 40 hr of integration time. *Top-left panel:* signal-to-noise ratio in the Si II absorption line as a function of pixel scale and galaxy J band apparent magnitude for the most compact galaxies ( $R_{half} = 100$  mas); *Bottom-left panel:* simulated integrated spectrum for a  $J_{AB} = 27$  galaxy. The red line represents the Shapley et al. (2003) input spectrum; *Middle panels* same results for a galaxy with average size ( $R_{half} = 150$  mas); *Right panel:* The black points represent the observed distribution of size ( $R_{half}$ ) vs. apparent J band magnitude in  $z \sim 7$  candidate galaxies from Grazian et al. (2012). The red squares represent the simulation grid, while the different color lines show the limiting magnitude at which one gets a signal-to-noise ratio of 10 per element of resolution in the Si II line as a function of pixel scale.

$z \sim 5$ . The velocity width was scaled so that the spatially integrated spectrum has a width  $\sigma = 270$  km/s, following measurements by Hu et al. (2010). Finally, we fold in the increasing correlation between the Ly- $\alpha$  equivalent width and UV-luminosity following the median relation found by Jiang et al. (2013). Results show that integration times of 10 hr will fulfil the requirement of detecting  $J_{AB} = 30$  LAEs with large enough signal to noise ratios (see Fig. 3). The optimal sampling is found to be 60-140 mas with no prefer value in this range, since variations of S/N can be easily compensated by tuning the relatively modest (for so distant sources) integration times.

## 6 Conclusion

The future 39m E-ELT will allow us to observe a large number of targets in its focal plane. To fully exploit such large target densities, one (or several) MOS will be required. We presented MOSAIC, which is a new international instrument study for an ELT-MOS. MOSAIC will offer a High Multiplex Mode with a large number of mono-aperture fibers, as well as a High Definition Mode, with  $\sim 10$  MOAO-fed IFUs, i.e., combining the best observational capabilities previously studied in the frame of the EAGLE and OPTIMOS-EVE Phase A instruments. We revisited the prominent science cases for the ELT-MOS, which were summarized in a White Paper and used to define the MOSAIC top level requirements. In order to assist the trade-off between these specifications, we conducted end-to-end simulations of some of these science cases. We argue that the best niche for ELT-MOS is to be optimized in term of survey speed (S/N), rather than in spatial resolution, which will be already provided by one of the two first light E-ELT instruments (ELT-IFU), although in a mono-object capability. The simulations conducted so far favor an IFU pixel scale of  $\sim 80$  mas, which allows reaching the scientific requirements on the detection of LAEs at least up to  $z \sim 9$ , and on the study of the galaxies ISM at  $z \sim 7$ . Further simulations will be required to investigate other driving science cases, such as the spatially-resolved properties of galaxies in absorption, the detection of very distant LBGs, as well as the limit and requirements of the High Multiplex Mode. Once completed, all these simulations will provide an extensive test-bench for assisting the trade-off between the MOSAIC top level requirements, and a comprehensive picture of the ELT-MOS scientific capabilities.

## References

- Bournaud, F., Elmegreen, B. G., & Elmegreen, D. M. 2007, *ApJ*, 670, 237
- Cuby, J.-G., Morris, S., Fusco, T., et al. 2010, in *Society of Photo-Optical Instrumentation Engineers (SPIE) Conference Series*, Vol. 7735, Society of Photo-Optical Instrumentation Engineers (SPIE) Conference Series
- Elmegreen, D. M., Elmegreen, B. G., Ravindranath, S., & Coe, D. A. 2007, *ApJ*, 658, 763
- Evans, C. J., Barbuy, B., Bonifacio, P., et al. 2012, in *Society of Photo-Optical Instrumentation Engineers (SPIE) Conference Series*, Vol. 8446, Society of Photo-Optical Instrumentation Engineers (SPIE) Conference Series
- Grazian, A., Castellano, M., Fontana, A., et al. 2012, *A&A*, 547, A51
- Hammer, F., Kaper, L., & Dalton, G. 2010, *The Messenger*, 140, 36
- Hammer, F., Puech, M., Assemat, F. F., et al. 2004, in *Society of Photo-Optical Instrumentation Engineers (SPIE) Conference Series*, Vol. 5382, Society of Photo-Optical Instrumentation Engineers (SPIE) Conference Series, ed. A. L. Ardeberg & T. Andersen, 727–736

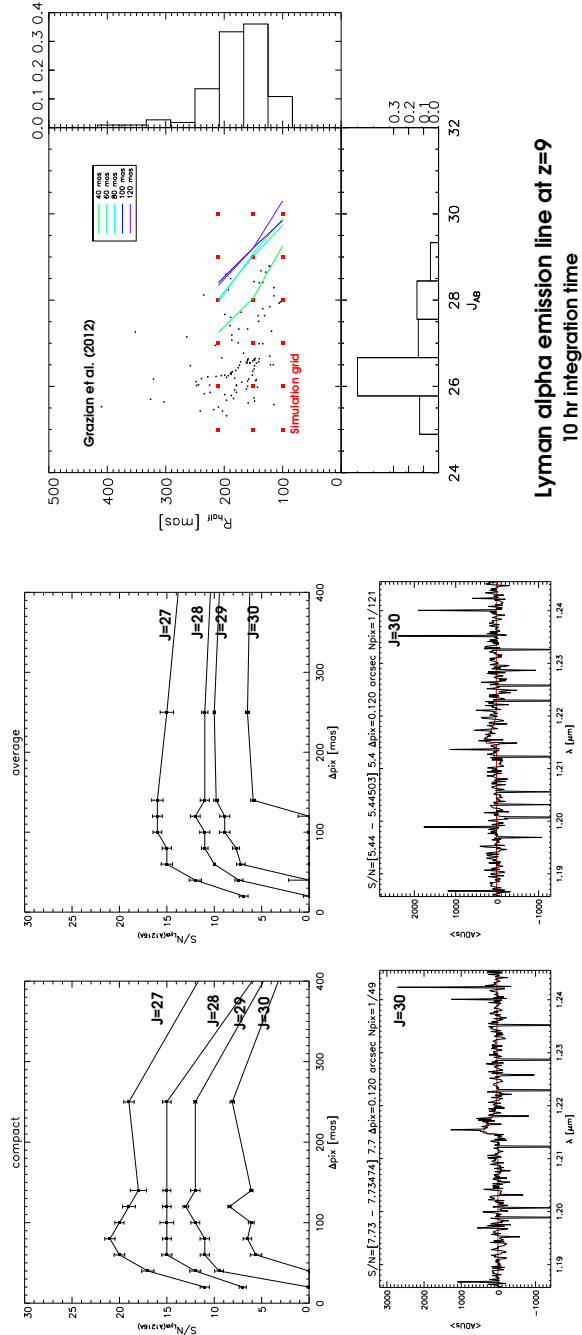


**Fig. 3.** Summary of the simulations of Ly- $\alpha$  emission line observations at  $z \sim 9$  with 10 hr of integration time. *Top-left panel:* signal-to-noise ratio in the Ly- $\alpha$  emission line as a function of pixel scale and galaxy J band apparent magnitude for the most compact galaxies ( $R_{half} = 100$  mas); *Bottom-left panel:* simulated integrated spectrum for a  $J_{AB} = 30$  galaxy. The red line represents the input template spectrum; *Middle panels* same results for a galaxy with average size ( $R_{half} = 150$  mas); *Right panel:* The black points represent the observed distribution of size ( $R_{half}$ ) vs. apparent J band magnitude in  $z \sim 7$  candidate galaxies from Grazian et al. (2012). The red squares represent the simulation grid, while the different color lines show the limiting magnitude at which one gets a signal-to-noise ratio of 10 per element of resolution in the Ly- $\alpha$  emission line as a function of pixel scale.

- Hu, E. M., Cowie, L. L., Barger, A. J., et al. 2010, *ApJ*, 725, 394
- Jiang, L., Egami, E., Mechtley, M., et al. 2013, *ApJ*, 772, 99
- Newman, S. F., Genzel, R., Förster Schreiber, N. M., et al. 2013, *ApJ*, 767, 104
- Puech, M. 2010, *MNRAS*, 406, 535
- Puech, M., Flores, H., Lehnert, M., et al. 2008, *MNRAS*, 390, 1089
- Puech, M., Lehnert, M., Yang, Y., et al. 2010a, in *Adaptive Optics for Extremely Large Telescopes*
- Puech, M., Rosati, P., Toft, S., et al. 2010b, *MNRAS*, 402, 903
- Puech, M., Yang, Y. B., & Flores, H. 2010c, in *Society of Photo-Optical Instrumentation Engineers (SPIE) Conference Series*, Vol. 7735, *Society of Photo-Optical Instrumentation Engineers (SPIE) Conference Series*
- Rosales-Ortega, F. F., Arribas, S., & Colina, L. 2012, *A&A*, 539, A73
- Shapley, A. E., Steidel, C. C., Pettini, M., & Adelberger, K. L. 2003, *ApJ*, 588, 65
- Steidel, C. C., Adelberger, K. L., Shapley, A. E., et al. 2003, *ApJ*, 592, 728
- Swinbank, A. M., Bower, R. G., Smith, G. P., et al. 2007, *MNRAS*, 376, 479